

3DSI Prostate Spectroscopy at 3T: Comparison of Multi-Element Coil Combinations

G. Metzger¹, S. Kozerke², J. Murdoch³, A-M. El-Sharkawy⁴, M. Bernardo⁵

¹Philips Medical Systems, Bethesda, MD, United States, ²Institute for Biomedical Engineering, University and Swiss Federal Institute of Technology Zurich, Zurich, Switzerland, ³Philips Medical Systems, Cleveland, OH, United States, ⁴Electrical and Computer Engineering, Johns Hopkins University, Baltimore, MD, United States, ⁵National Cancer Institute, National Institutes of Health, Bethesda, MD, United States

INTRODUCTION: MR spectroscopic imaging has been shown to aid in the early detection, staging and localization of prostate cancer. When investigating millimolar concentrations of metabolites in the prostate, an optimal combination of field strength, acquisition method, coil combination and reconstruction method is desired. The use of 3D spectroscopic imaging (3DSI) has been shown to be the acquisition method of choice in the prostate because of its inherently high SNR as well as its ability to selectively acquire data from the localized volume while allowing the needed multi-slice coverage [1]. With increased signal from higher static magnetic fields the possibility of using surface coils for such studies becomes realistic. Although some investigators have shown multi-element prostate spectroscopy work with surface coils [2,3], the typical coil configuration for prostate studies is a single element endorectal coil (ERC). In this work, 3 coil configurations are investigated with respect to their SNR when combined in an optimal reconstruction. We conclude that the best SNR relative gain is achieved by combining an ERC and a surface coil for acquiring 3DSI data in the prostate.

METHODS: The same volunteer was studied with all 3 coil configurations: a product 6 channel cardiac coil (CC), a 1.5T ERC alone (MRinnervu; Medrad, Pittsburgh, PA) and a combination of the ERC with 2 anterior surface elements (S+ERC), Figure 1. To use the Medrad ERC on the Philips 3T additional tuning and decoupling circuitry was constructed.

All spectroscopy studies were performed on a Philips Intera 3T (Philips Medical Systems, Best, The Netherlands). High bandwidth outer volume suppression bands were coincident with the borders of the PRESS box in-plane for the 3DSI acquisitions. Water suppression was accomplished with an optimized CHESSE pre-pulse and a BASING type pulse between the refocusing pulses [4]. Lipid suppression was accomplished with chemically shift selective adiabatic inversion with a sub-optimal delay of 220msec because of the other pre-pulses present. The SI field of view was encoded with a 12x12x12 matrix with an in-plane FOV of 10 cm for ERC coil combinations and 12cm for CC acquisitions. Both acquisitions used a slice thickness of 10 mm leading to a through plane FOV of 12 cm for all studies. Resulting nominal voxel sizes for the ERC coil configuration and CC acquisitions were 0.65 and 1.0 cc respectively. Other 3DSI parameters included TR/TE 960/100 msec, 60% scan percentage, transverse scan prescription and an acquisition time of 16:50.

The reconstruction was performed on the raw data in IDL (RSINC, Colorado). SI image generation, co-registration with anatomy and visualization was done in PRIDE (Philips Medical Systems, Cleveland, OH). All 3 spatial dimensions were processed with a hamming filter before applying the Fourier transform with no apodization in the temporal domain. 3DSI reconstruction was performed based on information intrinsic to the spatially localized data. The phase of each voxel was normalized by dividing the entire FID with the phase of the first time point while weighting factors for sum-of-squares reconstruction originated from the maximum magnitude signal found in the region of 2.0 to 3.5 ppm. Calculation of SNR was based on the signal strength of citrate at 2.6 ppm and the peak-to-peak noise in a region upfield from water.

RESULTS: The SNR for the CC channels 1 through 6 were 10, 27, 17, 16, 23 and 4 while the sum of squares SNR was 35. A 30% increase in SNR over the highest individual channel. The SNR for the ERC was 82 while the 2 surface coils had values of 15. The sum-of squares SNR for S+ERC was 84 resulting in a 2.5% improvement over the ERC alone. After normalizing for variable field homogeneities and nominal voxel sizes between the studies we find that the S+ERC SNR is increased by a factor of 3.17 times over that of the CC. Figures 2 and 3 show representative spectra from the S+ERC and CC respectively. The spectrum is superimposed on top of a T2W image from the same coil configuration demonstrating the PRESS volume and the voxel location of the displayed spectrum.

DISCUSSION: In this study, the surface coils used in combination with the ERC are not as efficient as the surface elements of the product cardiac coil. In addition, placement of the surface coils could also improve with elements both anterior and posterior. Channels 2 and 5 of the cardiac coil were positioned directly over the prostate on the anterior and posterior sides of the volunteer and exhibited nearly equivalent SNR. Multi-element ERCs would also benefit applications *in vivo* as already demonstrated in the canine prostate [5].

It is not surprising that the SNR of the S+ERC would have such a large advantage over the CC but the latter provides flexibility and ease of use in a clinical setting where the SNR increase of 3T can be traded off for sub-optimal coil configurations. Along with the ease of use of the CC, it has advantages when used for radiation therapy planning as it does not physically distort the prostate. Another advantage might be in the decreased spectral distortion caused by slight B1 effects near the elements of the ERC. A confounding factor to the use of surface coils alone is the variable performance depending on the size of the patient.

CONCLUSION: The S+ERC provides improved SNR over the CC or ERC alone. Future work will include optimization of S+ERC configurations to take full advantage of multi-coil 3DSI acquisitions at 3T.



Figure 1: CC (blue), S+ERC (yellow)

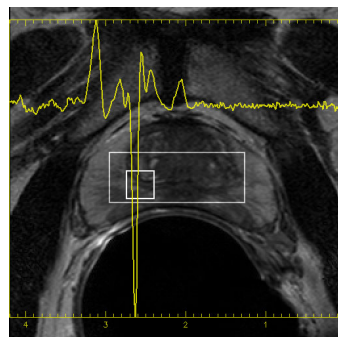


Figure 2: S+ERC spectrum (0.65 cc)

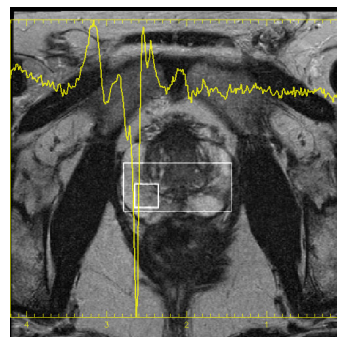


Figure 3: CC spectrum (1.0 cc)

REFERENCES: [1] Kurhanewicz J et al. Radiology 1996; 198:795-805 [2] Scheenen T et al. Proceedings of the 12th meeting of the ISMRM 2004; 612 [3] Mao H et al. Proceedings of the 12th meeting of the ISMRM 2004; 942 [4] Star L et al. MRM 1997;38:311-321 [5] Yung A et al. MRM 2003; 49:710-715